COMPARISON BETWEEN THE STIFFNESS METHOD AND THE HYBRID METHOD APPLIED TO A CIRCULAR RING

Nagore Insausti, Itziar Adarraga, Javier Urruzola, Faustino Mujika

Materials + Technologies Group / Mechanics of Materials, Department of Mechanical Engineering, Engineering Faculty of Gipuzkoa, University of the Basque Country (UPV/EHU)

Plaza de Europa, 1, 20018 Donostia-San Sebastián, Spain

E-mail: nagore.insausti@ehu.eus

ABSTRACT

This study deals with the comparison of stresses and displacements of a circular ring obtained by two numerical formulations, namely the Stiffness Method and the Hybrid Method, applied to isoparametric quadrilateral elements. After explaining the formulation of the hybrid method in finite elements, an orthogonalization method proposed previously for hybrid elements is applied. Then, the computational cost per element of the stiffness method and of the hybrid method with and without orthogonalization have been evaluated for the first time. A circular ring loaded by two opposing forces is analyzed in order to compare the solution obtained by the hybrid method and the stiffness method with experimental and analytical results. The agreement between analytical and experimental results with those numerical is better in the case of the hybrid method than in the case of the stiffness-method. It is observed that the element ratio needed to obtain a given relative error is one magnitude order greater in the stiffness method than in the case of the hybrid method.

Keywords: Force method; Stiffness method; Hybrid formulation; Circular ring

---

Nomenclature

$\{a^i\},\{a^t\}$	nodal displacements vector of the element and of the structure
a	thickness of the circular ring
A	cross sectional area of the circular ring

$[B]$	displacement-strain matrix
e	difference between the average radius and the radius of the neutral surface
$[E],[\bar{E}^*]$	equilibrium matrix
E	Young's modulus of material
$\{F^j\}$	stress parameters vector
$[G]$	flexibility matrix
G	shear modulus of material
I^*	equivalent moment of inertia
$[K^e],[K]$	SFM stiffness matrix of the element and of the structure
k	stiffness constant of the dynamometer
$[L]$	matrix of differential operators
M	bending moment
$[N]$	matrix of displacement interpolation functions
N	axial force
N_i	displacement interpolation functions
$\{P^i\},\{P^l\}$	external forces vector of the element and of the structure
P	concentrated force acting on the circular ring
r_i, r_o	inner and outer radius of the circular ring
(r, θ)	polar coordinates
R_a	average radius of the circular ring
R_e	radius of the neutral surface of the circular ring
$[S]$	compliance matrix of the material
t	element thickness
$\{u\}$	vector of displacements at any point in the element
U^*	complementary strain energy
X	the redundant unknown
$[Y]$	matrix of stress interpolation functions
δ	displacement
$\{\varepsilon\}$	strain field vector in element domain
ν	Poisson's ratio
ξ, η	natural coordinates

$\{\sigma_i\}$	stress field vector in element domain

1. Introduction

The Stiffness Method (SM) applied to finite element method (FEM) has been widely used in structural mechanics and mechanics of solids [1, 2].This method is derived from the application of the Principle of Virtual Work (PVW). In the SM a compatible displacement field is assumed in each element. The equilibrium conditions are considered in terms of nodal displacements that are the unknowns of the problem.

The other basic approach for structural analysis is the Force Method (FM) [2]. This method is derived from the application of the Principle of Complementary Virtual Work (PCVW), assuming an equilibrated stress field. Then, the compatibility equations are satisfied as a function of assumed stress parameters.

Fraeijs de Veubeke [3] showed that the SM and the FM are the lower and upper bounds of the exact solution, respectively. In the SM approach, all the admissible displacements of the system are not included. Therefore, the modeled system is more constrained than the actual case and the solution is over-stiff, being its energy a lower bound. In the FM all the admissible stresses of the system are not included, being the modeled system less constrained than the actual one. Thus, it is more flexible and its energy is an upper bound.

Regarding FM, Patnaik [4] formulated the Integrated Force Method (IFM) for discrete structures, introducing the use of both equilibrium equations and compatibility conditions. IFM and FM were compared analytically and numerically [5]. The advantage of IFM with respect to FM is that it is not necessary to select the redundant forces. Then, the governing equations of IFM can be directly automated for computer analysis. The formulation of IFM was extended for continuous systems in ulterior studies [6, 7]. New elements for finite element analysis via IFM have been proposed [8-13].

The Dual Integrated Force Method (IFMD) was also proposed by Patnaik *et al.* [14]. As IFMD is a dual form of IFM, both provide identical solutions for stresses and displacements. The formulation of IFMD is equivalent to that of IFM, but the structure of the governing equation of IFMD is similar to SM, as the primary unknowns of IFMD are the nodal displacements.

On the other hand, Pian [15] introduced the Hybrid Method (HM). Pian and Chen [16] proposed some alternative ways to formulate HM. Punch and Atluri [17] analyzed the stability and coordinate invariance of linear and quadratic serendipity hybrid stress elements. Pian [18] presented a review of the evolution of hybrid and mixed FEM. Wu and Cheung [19] proposed two approaches in order to improve the HM performance. Pian [20] pointed out some remarks on the first developments of the HM and proved the equivalence of the elements proposed by different authors.

HM are usually formulated based on the Hellinger-Reissner variational principle. Recently, Adarraga *et al*. [21] showed that this principle is equivalent to the application of the PVW and the PCVW which are equivalent to equilibrium and compatibility conditions, respectively. Therefore, the variational formulation of HM includes compatibility conditions, besides equilibrium conditions. In the same article, it has been shown that IFMD can be derived directly from the application of PVW and PCVW. The consequence is that IFMD and HM are equivalent. As they are based on the fulfillment of equilibrium equations as SM and compatibility conditions as FM, in the ensuing analysis the denomination Stiffness-Force Method (SFM) is used for the first time. It is worth noting that compatibility conditions are related to the fact that displacement and rotation fields are exact differentials [22]. That means that not only displacements, but also rotations are continuous single valued functions. Therefore, from a mathematical point of view, the continuity of third order derivatives of the displacements or C^3 continuity is required [23, 24]. Nevertheless, in the formulation of quadrilateral elements by SM only the continuity of displacements or C^0 continuity is required. One of the significant issues regarding SFM is the selection of the assumed optimal stress modes [25-29]. Zhang *et al*. [30] proposed a method to determine the assumed stress modes free of spurious zero energy modes, based on the basic orthogonal deformation modes. Recently, a new method to select the optimal stress field in a systematic and quantitative way has been developed [31].

Furthermore, in SFM the inversion of the flexibility matrix to compute the stiffness matrix is required, increasing the computational cost. In order to minimize the computational requirements, Saether [32, 33] proposed an explicit formulation. Zhang *et al*. [34, 35] suggested an orthogonalization method based on the definition of an inner product.

The aim of the present study is to compare SFM with SM in the case of general quadrilateral elements. With this purpose, the formulation of SFM has been briefly reviewed and the orthogonalization method proposed by Zhang *et al*. [35] has been applied. Then, an analysis of the computational cost of each element in the different FEM formulations has been carried out. A circular ring acted on by two opposing forces is analyzed. This problem has been selected because experimental results of stiffness concerning a commercial dynamometer are available. Moreover, analytical results are determined by applying the theorem of Engesser-Castigliano [36]. Finally, numerical results obtained by SFM and SM are compared with experimental and analytical results.

2. Stiffness-Force Method

2.1. Formulation

SFM is developed based on PVW and PCVW. Displacements and stresses are interpolated separately and the governing equation has the nodal displacements as unknowns. Stresses are not obtained from the constitutive relations after differentiating the displacements in order to determine strains, but they are obtained directly from stress parameters. Usually, the absence of numerical differentiation of displacements is argued as the reason for obtaining better results in SFM. Nevertheless, from our point of view the fact of having introduced compatibility conditions by means of PCVW in the formulation is other important factor.

According to PVW [37] and assuming that each element has n_e independent displacements, the virtual work done by the external forces in an element is equal to the virtual work of the stresses:

$$\int_V \left\{\delta\varepsilon\right\}^T \left\{\sigma\right\} dV = \left\{\delta a^i\right\}^T \left\{P^i\right\} \tag{1}$$

Where V is the volume of the element; $\{\delta\varepsilon\}$ and $\{\delta a^i\}$ are the virtual strain and nodal displacement vectors; $\{\sigma\}$ is the stress vector; $\{P^i\}$ is the nodal external forces vector; and i = 1 to n_e are the displacement degrees of freedom of the element.

The displacements $\{u\}$ at any point of the element are calculated from the nodal displacements by means of the interpolation functions of SM:

$$\{u\} = [N]\{a^i\} \tag{2}$$

Where $\{a^i\}$ is the nodal displacements vector and $[N]$ is the matrix of displacement interpolation functions.

Element displacements $\{u\}$ are related to the strains $\{\varepsilon\}$ through the matrix of differential operators $[L]$:

$$\{\varepsilon\} = [L]\{u\} \tag{3}$$

Therefore, replacing Eq. (2) in Eq. (3), the strains $\{\varepsilon\}$ can be related directly to the nodal displacements $\{a^i\}$:

$$\{\varepsilon\} = [L][N]\{a^i\} = [B]\{a^i\} \tag{4}$$

Where $[B]$ is the nodal displacement-strain matrix.

In SFM, an independent stress field is also adopted. Considering that each element has m_e independent stress modes, the stresses $\{\sigma\}$ at any point of the element are interpolated in terms of the stress parameters $\{F^j\}$ [21]:

$$\{\sigma\} = [Y]\{F^j\} \tag{5}$$

Where $[Y]$ is the matrix of stress interpolation functions and $\{F^j\}$ are the stress parameters, with j = 1 to m_e.

The stress interpolation functions are formulated from the stress functions that are derived from complete polynomials [2] that satisfy equilibrium equations. Replacing Eqs. (4) and (5) in Eq. (1), it results:

$$\left\{\delta a^i\right\}^T \left(\int_V \left[B\right]^T \left[Y\right] dV\right) \left\{F^j\right\} = \left\{\delta a^i\right\}^T \left\{P^i\right\} \tag{6}$$

As $\left\{\delta a^i\right\}$ are arbitrary, the equilibrium Eq. (6) can be written as follows:

$$\left[E\right]\left\{F^j\right\} = \left\{P^i\right\} \tag{7}$$

Where $\left[E\right]$ is the element equilibrium matrix of order n_e x m_e, defined as:

$$\left[E\right] = \int_V \left[B\right]^T \left[Y\right] dV \tag{8}$$

Otherwise, the PCVW [37] states that:

$$\int_V \left\{\delta\sigma\right\}^T \left\{\varepsilon\right\} dV = \left\{\delta P^i\right\}^T \left\{a^i\right\} \tag{9}$$

Where $\left\{\delta\sigma\right\}$ and $\left\{\delta P^i\right\}$ are the virtual stress and external forces vectors.

Taking into account the relation between strains $\left\{\varepsilon\right\}$ and stresses $\left\{\sigma\right\}$:

$$\left\{\varepsilon\right\} = \left[S\right]\left\{\sigma\right\} \tag{10}$$

Where $\left[S\right]$ is the compliance matrix of the material. Replacing Eqs. (5), (7) and (10) in Eq. (9), it results:

$$\left\{\delta F^j\right\}^T \left(\int_V \left[Y\right]^T \left[S\right]\left[Y\right] dV\right) \left\{F^j\right\} = \left\{\delta F^j\right\}^T \left[E\right]^T \left\{a^i\right\} \tag{11}$$

As $\left\{\delta F^j\right\}$ are arbitrary, Eq. (11) can be written as follows:

$$\left[G\right]\left\{F^j\right\} = \left[E\right]^T \left\{a^i\right\} \tag{12}$$

Where $\left[G\right]$ is the flexibility matrix of the element, defined as:

$$\left[G\right] = \int_V \left[Y\right]^T \left[S\right]\left[Y\right] dV \tag{13}$$

The stress parameters $\left\{F^j\right\}$ of the element are obtained from Eq. (12), being:

$$\left\{F^j\right\} = \left[G\right]^{-1} \left[E\right]^T \left\{a^i\right\} \tag{14}$$

Now, replacing Eq. (14) in the equilibrium equation defined in Eq. (7), it gives:

$$\left\{P^i\right\} = \left(\left[E\right]\left[G\right]^{-1}\left[E\right]^T\right)\left\{a^i\right\} \tag{15}$$

Equation (15) can be written as:

$$\left[K^e\right]\left\{a^i\right\} = \left\{P^i\right\} \tag{16}$$

Where $\left[K^e\right]$ is the SFM stiffness matrix of the element given by:

$$\left[K^e\right] = \left[E\right]\left[G\right]^{-1}\left[E\right]^T \tag{17}$$

The stiffness matrix of the structure $\left[K\right]$ is obtained by the assembly of the elemental stiffness matrices like in the case of SM. Hence, the governing equation of SFM is:

$$\left[K\right]\left\{a^l\right\} = \left\{P^l\right\} \tag{18}$$

Where l = 1 to n_s and k = 1 to m_s, being n_s and m_s the degrees of freedom of displacements and forces of the complete system, respectively.

Once the nodal displacements are known the stress parameters are obtained from Eq. (14) and the stresses $\left\{\sigma\right\}$ at any point of the element are determined by Eq. (5). The strains $\left\{\varepsilon\right\}$ are obtained from strain-stress relation of Eq. (10).

One of the main drawbacks of SFM is the requirement of determining the inverse of the flexibility matrix [G] to compute the stiffness matrix. In this way, different approaches have been proposed to improve the computational efficiency of SFM [32-35].

2.2. Quadrilateral elements

In this section, interpolation functions of forces and displacements of an isoparametric quadrilateral element shown in Fig. 1 are described [26]. The displacement interpolation functions are the same as those used in SM:

$$\begin{aligned} u &= \sum_{i=1}^{4} N_i u_i = \frac{1}{4}\sum\left(1+\xi\xi_i\right)\left(1+\eta\eta_i\right)u_i \\ v &= \sum_{i=1}^{4} N_i v_i = \frac{1}{4}\sum\left(1+\xi\xi_i\right)\left(1+\eta\eta_i\right)v_i \end{aligned} \tag{19}$$

Where ξ_i and η_i are the natural nodal coordinates.

Using the stress interpolation functions defined in [26, 35] for the four-node isoparametric quadrilateral element, Eq. (5) can be written as:

$$\begin{Bmatrix} \sigma_x \\ \sigma_y \\ \tau_s \end{Bmatrix} = \frac{1}{t} \begin{Bmatrix} N_x \\ N_y \\ N_s \end{Bmatrix} = \frac{1}{t} \begin{bmatrix} 1 & 0 & 0 & a_1^2\eta & a_3^2\xi \\ 0 & 1 & 0 & b_1^2\eta & b_3^2\xi \\ 0 & 0 & 1 & a_1 b_1\eta & a_3 b_3\xi \end{bmatrix} \begin{Bmatrix} F_1 \\ F_2 \\ F_3 \\ F_4 \\ F_5 \end{Bmatrix} \tag{20}$$

Zhang *et al.* [34, 35] proposed an orthogonalization method to avoid the determination of the inverse of [G]. Moreover, they carried out an explicit formulation in order to obtain the stiffness matrix of quadrilateral hybrid stress elements.

2.3. Number of floating-point operations

Considering the same number of elements in SM and SFM, the global stiffness matrix is of the same order in both cases. Then, the main difference between them is the construction of the stiffness matrix of each element. Table 1 shows the computational cost for the stiffness matrix of 2D four-node isoparametric element in three cases:

- Basic SFM without diagonalization and with numerical integration
- SFM formulated in explicit manner according to the orthogonalization proposed in [34, 35]
- SM with numerical integration

Table 1. FLOPs concerning the calculation of the stiffness matrix of the 2D 4-node isoparametric element.

Step	Basic SFM	SFM explicit formulation	SM
$[E]$ and $[G]$ [a]	2179	-	-
$[\bar{E}^*]$ [b]	-	289	-
$[K]$ [c]	579	360	1766
TOTAL	**2758**	**649**	**1766**

[a]Basic SFM: Eq. (8) and Eq. (13), integration with 4 Gauss points, one matrix product (8x3, 3x5), one matrix product (5x3, 3x3), one symmetric product (5x3, 3x5); SFM explicit and SM: not applicable.

[b]SFM explicit: see [35]; Basic SFM and SM: not applicable.

[c]Basic SFM: Eq. (17), inverse by Cholesky (5x5), one triangular back substitution and one matrix product (5x5, 5x8), one symmetric product (8x5, 5x8); SFM explicit: see [35], one symmetric product (8x5, 5x8); SM: integration with 4 Gauss points, one matrix product (8x3, 3x3), one symmetric product (8x3, 3x8).

Figure 2 is a symbolic representation of the FLOP comparisons shown in Table 1. The saving of the computational cost concerning the explicit formulation of SFM is 60 % with respect to SM and 75 % with respect to Basic SFM.

Otherwise, the formulation used to compute stresses is different in SFM and SM. Table 2 shows the computational cost of stress calculation for 2D four-node isoparametric element in the same cases as in Table 1.

Table 2. FLOPs concerning the calculation of stresses of the 2D 4-node isoparametric element.

Step	Basic SFM	SFM explicit formulation	SM
$\left\{F^{j}\right\}$ [a]	2702	369	-
$\left\{\varepsilon\right\}$ [b]	-	-	572
$\left\{\sigma\right\}$ [c]	240	393	60
TOTAL	**2942**	**762**	**632**

[a]Basic SFM: Eq. (14), repeated calculation of $[E]$ and $[G]$, inverse by Cholesky (5x5), two matrix products (5x5, 5x5 and 5x5, 5x8), one matrix-vector product (5x8, 8); SFM explicit: see [35], repeated calculation of $\left[\overline{E}^{\cdot}\right]$, one matrix-vector product (5x8, 8); SM: not applicable.

[b]SM: one matrix-vector product (3x8, 8); Basic SFM and SFM explicit: not applicable.

[c]Basic SFM and SFM explicit: Eq. (5) and see [35], one matrix-vector product (3x5, 5); SM: one matrix-vector product (3x3, 3).

Figure 3 is a symbolic representation of the FLOP comparisons shown in Table 2. The saving of the computational cost of SFM with explicit formulation with respect to Basic SFM is 70 %. The reduction of the computational cost of SM with respect to SFM explicit is 20 %.

If the differences in the calculation of the stiffness matrix and the stresses are added, the saving of computational cost of the explicit SFM with respect to SM is approximately 40 % and with respect to Basic SFM it is 75 %.

3. Analytic approach of a circular ring acted on by two forces

3.1. Circumferential stresses

A scheme of the circular ring under study is shown in Fig. 4. The outer radius of the circular ring is represented by r_o and the inner radius by r_i. The cross section of the ring is rectangular, its thickness is defined as a and its width as t. According to the approach of Winkler for curved bars [36, 38], the circumferential normal stress distribution is given by:

$$\sigma_\theta = \frac{N}{A} + \frac{M\left(r - R_e\right)}{Aer} \tag{21}$$

Being (r, θ) the polar coordinates; N the axial force; A the cross sectional area; M the resultant moment; $R_e = a/\left(\ln r_o/r_i\right)$ the radius of the neutral surface; $e = R_a - R_e$ the difference between the average radius and the radius of the neutral surface and $R_a = r_o + a/2$ the distance from O to the centroid of the cross section.

In curved beams significant radial stresses can be developed owing to the initial curvature of the beam. These radial stresses are inversely proportional to the radius of curvature of the beam, r [36]. As in the case under study the radius of curvature is large, radial stresses σ_r and shear stresses $\tau_{r\theta}$ are assumed to be negligible compared with circumferential stresses σ_θ.

3.2. Displacements

In order to calculate displacements, the theorem of Engesser-Castigliano is used. As a first approach, the effect of radial stresses is neglected and that concerning shear stresses is introduced assuming that they have a parabolic distribution through the thickness. As a consequence, the value of shear factor 6/5 corresponding to straight beams is used. Thus, the derivative of the complementary strain energy with respect to a force F_i is given by:

$$\frac{\partial U^*}{\partial F_i} = \int_L \frac{MM'}{EI^*} dl + \int_L \frac{NN'}{EA} dl + \tfrac{6}{5} \int_L \frac{VV'}{GA} dl \tag{22}$$

Being : $I^* = \dfrac{A^2 e^2}{R_e{}^2 \beta - A} \quad \beta = \dfrac{ta}{r_i r_o}$

These parameters are a consequence of the hyperbolic distribution of circumferential stresses of Winkler's approach, given in Eq. (21).

After having determined the internal forces and moments, the vertical displacement at *B* can be computed using Eq. (22):

$$\delta_B = \left(\frac{-1}{\pi} + \frac{\pi}{8} \right) \frac{PR_a{}^3}{EI^*} + \frac{\pi}{8} \frac{PR_a}{EA} + \frac{3\pi}{20} \frac{PR_a}{GA} \tag{23}$$

The relative displacement between points *B* and *C* of Fig. 4 is $\delta_{BC} = 2\delta_B$.

4. Analytic, numerical and experimental results

4.1. Displacements

The circular dynamometer of rectangular cross section shown in Fig. 5 has been analyzed. Experimental load-displacement data provided by the manufacturer CONTROLS will be used for comparative purposes [39]. The geometrical features and the elastic properties provided by the manufacturer are:

r_o = 91 mm, r_i = 78 mm, a = 13 mm and t = 51 mm

E = 210 GPa, G = 80.8 GPa and ν = 0.3.

The load-displacement relationship provided by the manufacturer is linear. The values of the stiffness *k* of the dynamometer determined experimentally, analytically, and numerically by SM and SFM are shown in Table 3. The numerical results have been obtained with a mesh of 48 elements. The values obtained by SFM are closer to the experimental value and the analytical approach than that given by SM.

The analytic value of the stiffness obtained from Eq. (23) agrees with the experimental one, being the relative error 0.8%. Therefore, hereinafter numerical and analytical results will be compared.

Table 3. Stiffness constant k of the dynamometer in N/mm

	Experimental	Analytical approach	SFM	SM
k(N/mm)	20756	20914	21385	27223

The displacements of the dynamometer have been determined numerically by SM and SFM, both implemented in MATLAB. The problem has been solved with different meshes of 2D 4-noded quadrilateral elements. Figure 6 shows the model carried out with 48 elements.

Figure 7 shows the values of the normalized displacements with respect to analytical values for different meshes obtained by SFM and SM. The convergence to the analytic approach is faster with SFM solution than with SM.

The relative errors with respect to those analytical are shown in Fig. 8. The relative error for a mesh of 48 elements obtained by SFM for displacements is close to 2%. In order to obtain that relative error by SM it is necessary a mesh of 1200 elements. It is apparent that in the current example the computational cost is not an issue. Nevertheless, besides the low computational cost per element pointed out previously, the model needed is 25 times coarser in order to get the same error. In other words, it is possible to model larger systems for the same computational cost in the case of plane problems that include bending.

4.2. Stresses

The experimental value of the stiffness constant of the dynamometer is given by the manufacturer and the analytical value is obtained from the complementary strain energy, based on the stress distribution. Furthermore, experimental and analytical displacement results agree. As the stress field of Eq. (21) leads to correct displacements, the analytical stress distribution is considered suitable and the numerical results will be compared with respect to it.

Figure 9 shows circumferential stresses of section *A* of Fig. 4 at the inner and outer radius of the dynamometer obtained by SFM and SM for different meshes. The convergence is faster for SFM than for SM. Figure 10 shows the distribution of circumferential stresses along the thickness of section *A* for a mesh of 48 elements. SFM results agree better with the analytical approach than the stresses given by SM. The relative errors with respect to values obtained by Eq. (21) are shown in Fig. 11. In the case of SFM that error is less than 2 % at the inner and outer radius. In order to obtain that relative error by SM it is necessary a mesh of 600 elements. Therefore, in the case of stresses the model needed is 12 times coarser in order to get the same error.

5. Summary and conclusions

The FEM has been implemented in 2D four-node isoparametric quadrilateral elements using the hybrid formulation, namely Stiffness Force Method, that is based on the two fundamental principles of virtual work.

An analysis of the number of FLOPs of the Stiffness Method and the Stiffness Force Method has been carried out. Explicit SFM is the method with the lowest computational cost.

A circular ring acted on by two opposing forces has been analyzed analytically and numerically by SM and SFM. The analytic approach in displacements has been verified by comparing it with experimental data. The numerical results show that the displacements and stresses obtained by SFM converge faster to analytical results than those obtained by SM. Moreover, it is observed that the number of elements needed to obtain a given relative error is much greater in the case of SM than in SFM. Therefore, using SFM, besides the improvement in computational cost per element, the number of elements for a given model could be significantly reduced.

Acknowledgements

The financial support of the University of the Basque Country (UPV/EHU) in the Research Group GIU 16/51 "Mechanics of Materials" is gratefully acknowledged.

References

1. Oñate E (2009) Structural Analysis with the Finite Element Method. International Center for Numerical Methods in Engineering, Barcelona.

2. Robinson J (1973) Integrated Theory of Finite Element Methods. John Wiley & Sons, London.

3. Zienkiewicz OC (2001) Displacement and equilibrium models in the finite element method by B. Fraeijs de Veubeke, Chapter 9, Pages 145–197 of Stress Analysis, Edited by O. C. Zienkiewicz and G. S. Holister, Published by John Wiley & Sons, 1965. Int J Numer Methods Eng 52:287-342. doi: 10.1002/nme.339.

4. Patnaik S (1973) An integrated force method for discrete analysis. Int J Numer Methods Eng 6:237-251. doi: 10.1002/nme.1620060209.

5. Patnaik SN (1986) The integrated force method versus the standard force method. Comput Struct 22:151-163. doi: http://dx.doi.org/10.1016/0045-7949(86)90061-1.

6. Patnaik SN, Nagaraj MS (1987) Analysis of continuum by the integrated force method 26:899-905. doi: http://dx.doi.org/10.1016/0045-7949(87)90106-4.

7. Patnaik SN, Satish HG (1990) Analysis of continuum using boundary compatibility conditions of integrated force method 34:287-295. doi: http://dx.doi.org/10.1016/0045-7949(90)90372-9.

8. Dhananjaya HR, Nagabhushanam J, Pandey PC (2007) Bilinear plate bending element for thin and moderately thick plates using Integrated Force Method. Struct Eng Mech 26:43-68

9. Dhananjaya HR, Nagabhushanam J, Pandey PC (2008) Automatic generation of equilibrium and flexibility matrices for plate bending elements using Integrated Force Method. Struct Eng Mech 30:387-402

10. Dhananjaya HR, Pandey PC, Nagabhushanam J (2009) New eight node serendipity quadrilateral plate bending element for thin and moderately thick plates using Integrated Force Method. Struct Eng Mech 33:485-502

11. Dhananjaya HR, Nagabhushanam J, Pandey PC, Jumaat MZ (2010) New twelve node serendipity quadrilateral plate bending element based on Mindlin-Reissner theory using Integrated Force Method. Struct Eng Mech 36:625-642

12. Dhananjaya HR, Pandey PC, Nagabhushanam J, Othamon I (2011) Closed form solutions for element equilibrium and flexibility matrices of eight node rectangular plate bending element using integrated force method. Struct Eng Mech 40:121-148

13. Dhananjaya HR, Pandey PC, Nagabhushanam J, Ibrahim Z (2012) New nine-node Lagrangian quadrilateral plate element based on Mindlin-Reissner theory using IFM. Struct Eng Mech 41:205-229

14. Patnaik SN, Coroneos RM, Hopkins DA (1998) Recent advances in the method of forces: integrated force method of structural analysis. Adv Eng Software 29:463-474. doi: http://dx.doi.org/10.1016/S0965-9978(97)00070-7.

15. Pian THH (1964) Derivation of Element Stiffness Matrices by Assumed Stress Distributions. AIAA J 2:1333-1336

16. Pian THH, Chen D (1982) Alternative ways for formulation of hybrid stress elements. Int J Numer Methods Eng 18:1679-1684. doi: 10.1002/nme.1620181107.

17. Punch EF, Atluri SN (1984) Development and testing of stable, invariant, isoparametric curvilinear 2- and 3-D hybrid-stress elements. Comput Methods Appl Mech Eng 47:331-356. doi: http://dx.doi.org/10.1016/0045-7825(84)90083-5.

18. Pian THH (1995) State-of-the-art development of hybrid/mixed finite element method 21:5-20. doi: http://dx.doi.org/10.1016/0168-874X(95)00024-2.

19. Wu C, Cheung YK (1995) On optimization approaches of hybrid stress elements 21:111-128. doi: http://dx.doi.org/10.1016/0168-874X(95)00023-0.

20. Pian THH (2000) Some notes on the early history of hybrid stress finite element method. Int J Numer Methods Eng 47:419-425. doi: 10.1002/(SICI)1097-0207(20000110/30)47:1/3<419::AID-NME778>3.0.CO;2-#.

21. Adarraga I, Cantera MA, Romera JM, Insausti N, Mujika F (2014) The dual integrated force method applied to unidirectional composites. Int J Numer Methods Eng 98:663-677. doi: 10.1002/nme.4644.

22. Love AEH (1944) A treatise on the mathematical theory of elasticity. Dover, New York.

23. Sokolnikoff IS (1956) Mathematical theory of elasticity. McGraw-Hill Book, New York.

24. Muskhelishvili NI (1977) Some basic problems of the mathematical theory of elasticity :fundamental equations plane theory of elasticity torsion and bending. Noordhoff, Groningen.

25. Pian THH, Chen D (1983) On the suppression of zero energy deformation modes. Int J Numer Methods Eng 19:1741-1752. doi: 10.1002/nme.1620191202.

26. Pian THH, Sumihara K (1984) Rational approach for assumed stress finite elements. Int J Numer Methods Eng 20:1685-1695. doi: 10.1002/nme.1620200911.

27. Kaljević I, Patnaik SN, Hopkins DA (1996) Development of finite elements for two-dimensional structural analysis using the integrated force method. Comput Struct 59:691-706. doi: http://dx.doi.org/10.1016/0045-7949(95)00294-4.

28. Kaljević I, Patnaik SN, Hopkins DA (1996) Three-dimensional structural analysis by the integrated force method. Comput Struct 58:869-886. doi: http://dx.doi.org/10.1016/0045-7949(95)00171-C.

29. Feng W, Hoa SV, Huang Q (1997) Classification of stress modes in assumed stress fields of hybrid finite elements. Int J Numer Methods Eng 40:4313-4339. doi: 10.1002/(SICI)1097-0207(19971215)40:23<4313::AID-NME259>3.0.CO;2-N.

30. Zhang C, Wang D, Li T (2011) Orthogonal basic deformation mode method for zero-energy mode suppression of hybrid stress elements 32:83-96. doi: 10.1007/s10483-011-1396-6.

31. Zhang C, Hoa SV (2014) A systematic and quantitative method to determine the optimal assumed stress fields for hybrid stress finite elements. Finite Elements Anal Des 80:41-62. doi: http://dx.doi.org/10.1016/j.finel.2013.10.008.

32. Saether E (1995) Explicit determination of element stiffness matrices in the hybrid stress method. Int J Numer Methods Eng 38:2547-2571. doi: 10.1002/nme.1620381505.

33. Saether E (1996) An explicit plane quadrilateral element for nonlinear material analysis. Comput Struct 61:529-538. doi: http://dx.doi.org/10.1016/0045-7949(96)00062-4.

34. Zhang CH, Feng W, Huang Q (2002) The stress subspace of hybrid stress element and the diagonalization method for flexibility matrix H 23:1263-1273

35. Zhang C, Wang D, Zhang J, Feng W, Huang Q (2007) On the equivalence of various hybrid finite elements and a new orthogonalization method for explicit element stiffness formulation. Finite Elements Anal Des 43:321-332. doi: http://dx.doi.org/10.1016/j.finel.2006.11.002.

36. Oden JT, Ripperger EA (1981) Mechanics of Elastic Structures. Hemisphere Publishing Corporation, Washington.

37. Shames IH, Dym CL (1985) Energy and Finite Element Methods in Structural Mechanics. Hemisphere Publishing Corporation, New York.

38. Beer FP, Johnston Jr. ER, Dewolf JT, Mazurek DF (2012) Mechanics of materials. McGraw-Hill, New York.

39. Controls Group. http://www.controls-group.com/eng/universal-testers-_-steel-re_bars-testing-equipment/universal-load-frames-accessories-for-soil-asphalt-concrete-cement-mortar-and-rock-testings.php

Figure captions

Fig. 1 The 2D four-node isoparametric quadrilateral element: (a) global coordinates; (b) natural coordinates

Fig. 2 FLOP comparisons for constructing the stiffness matrix

Fig. 3 FLOP comparisons for obtaining the stresses

Fig. 4 Scheme of the circular ring

Fig. 5 Circular dynamometer

Fig. 6 Coordinate system, discretization, loading and boundary conditions of the 48 elements FEM model of the circular ring

Fig. 7 Vertical displacement at B obtained with SFM and SM normalized with respect to analytical values

Fig. 8 Relative error of the vertical displacement at B with respect to analytical values

Fig. 9 FEM results of the stresses at *A*, normalized with respect to analytical values: (a) at the inner radius; (b) at the outer radius

Fig. 10 Analytical and FEM solutions of the stresses throughout the thickness at *A*, for 48 elements

Fig. 11 Relative error estimation of the stresses at A with respect to analytical approach: (a) at the inner radius, (b) at the outer radius

Figure captions

Fig. 1 The 2D four-node isoparametric quadrilateral element: (a) global coordinates; (b) natural coordinates

Fig. 2 FLOP comparisons for constructing the stiffness matrix

Fig. 3 FLOP comparisons for obtaining the stresses

Fig. 4 Scheme of the circular ring

Fig. 5 Circular dynamometer

Fig. 6 Coordinate system, discretization, loading and boundary conditions of the 48 elements FEM model of the circular ring

Fig. 7 Vertical displacement at B obtained with SFM and SM normalized with respect to analytical values

Fig. 8 Relative error of the vertical displacement at B with respect to analytical values

Fig. 9 FEM results of the stresses at *A*, normalized with respect to analytical values: (a) at the inner radius; (b) at the outer radius

Fig. 10 Analytical and FEM solutions of the stresses throughout the thickness at *A*, for 48 elements

Fig. 11 Relative error estimation of the stresses at A with respect to analytical approach: (a) at the inner radius, (b) at the outer radius

Figure 1

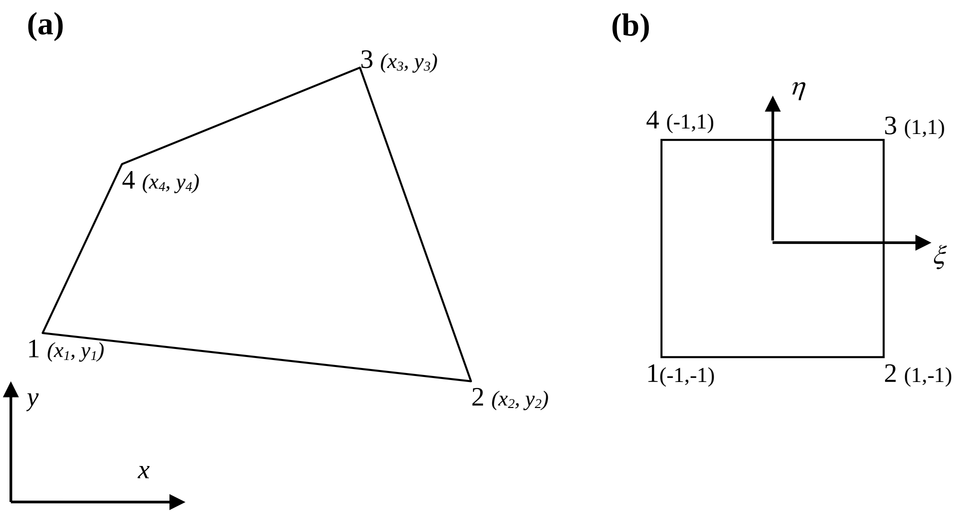

Figure 2

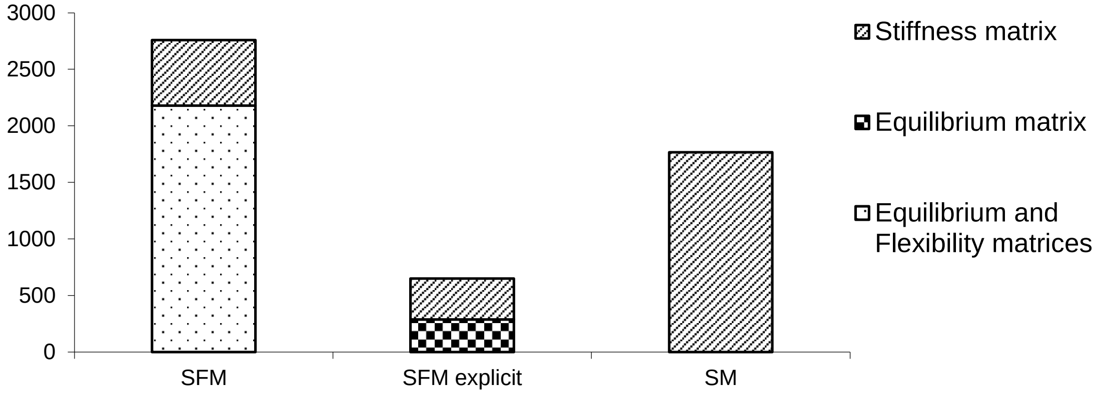
3000
2500
2000
1500
1000
500
0
SFM
SFM explicit
SM
Stiffness matrix
Equilibrium matrix
Equilibrium and Flexibility matrices

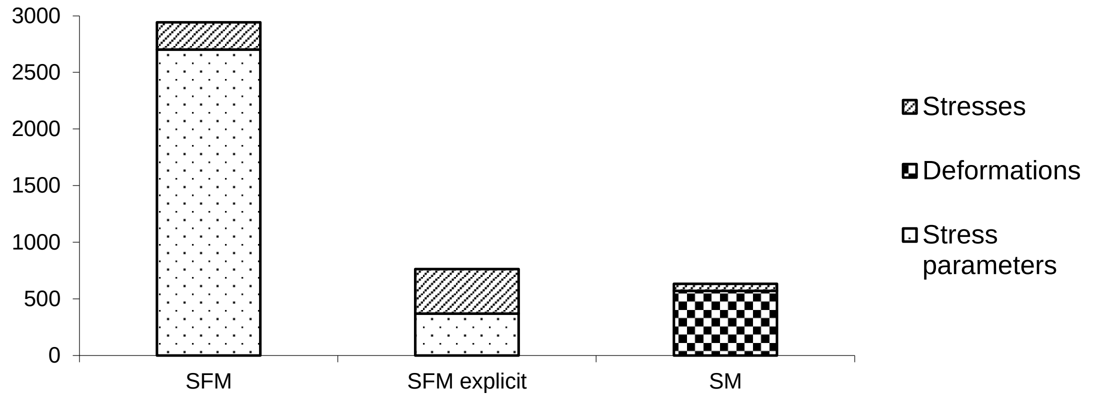
3000
2500
2000
1500
1000
500
0
SFM
SFM explicit
SM
Stresses
Deformations
Stress parameters

Figure 4

Click here to download Figure FIG4.DOC.docx

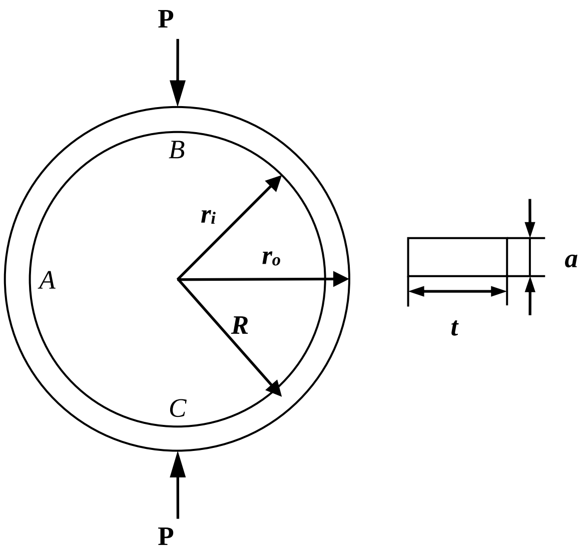

Figure 5

Click here to download Figure FIG5.TIF

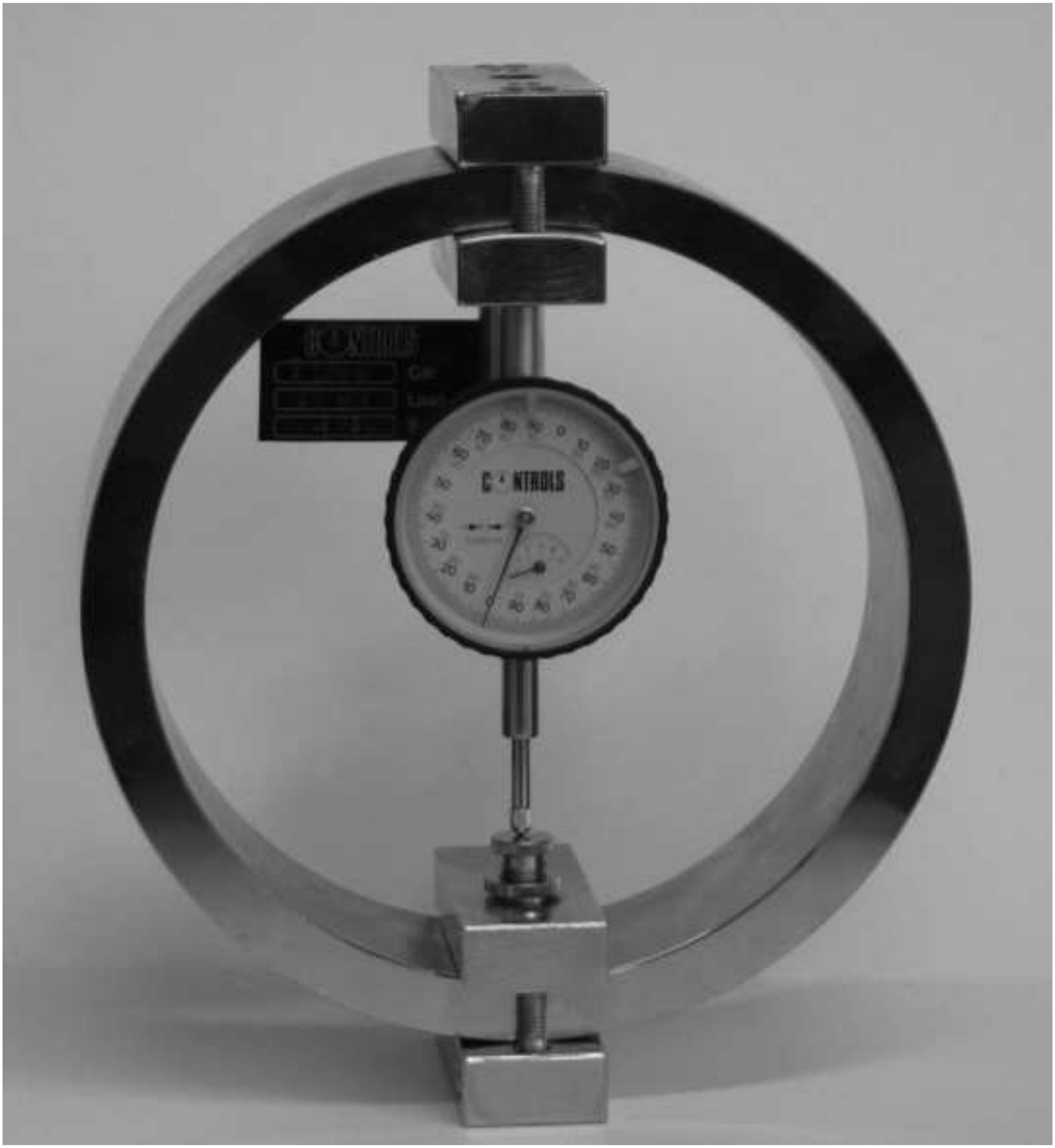

Figure 6

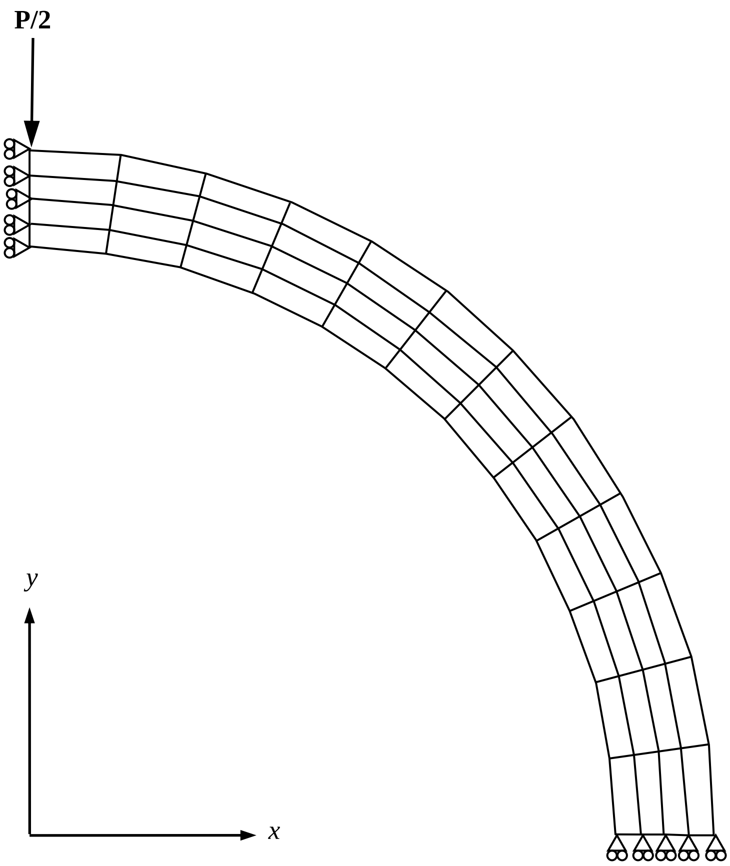

Figure 7

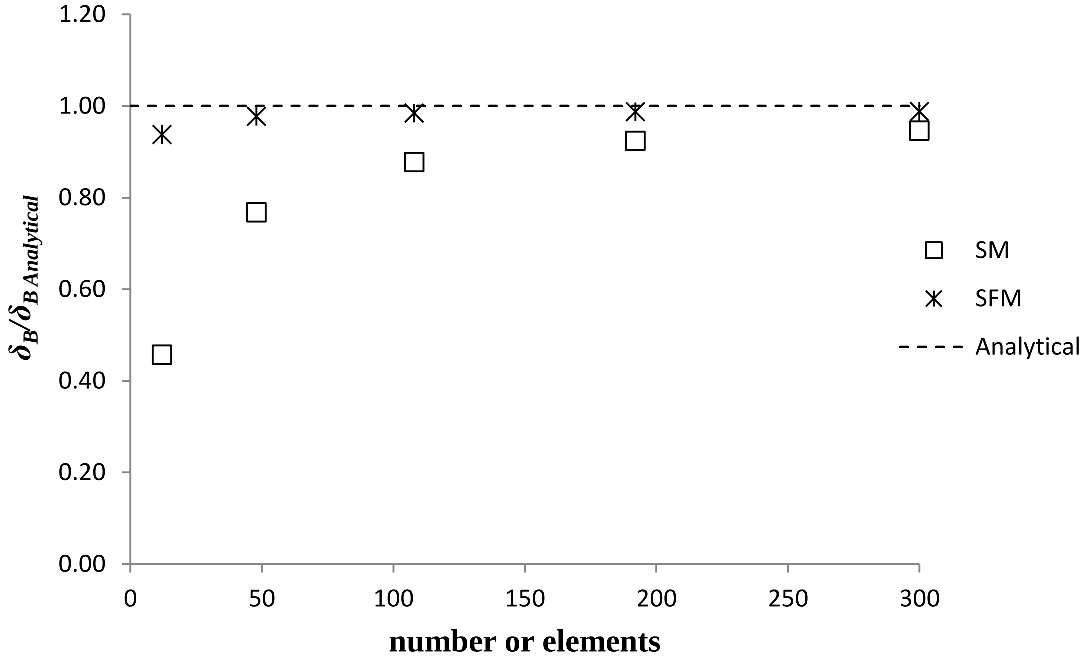
1.20
1.00
0.80
0.60
0.40
0.20
0.00
0
50
100
150
200
250
300
$\delta_B/\delta_{B\,Analytical}$
number or elements
SM
SFM
Analytical

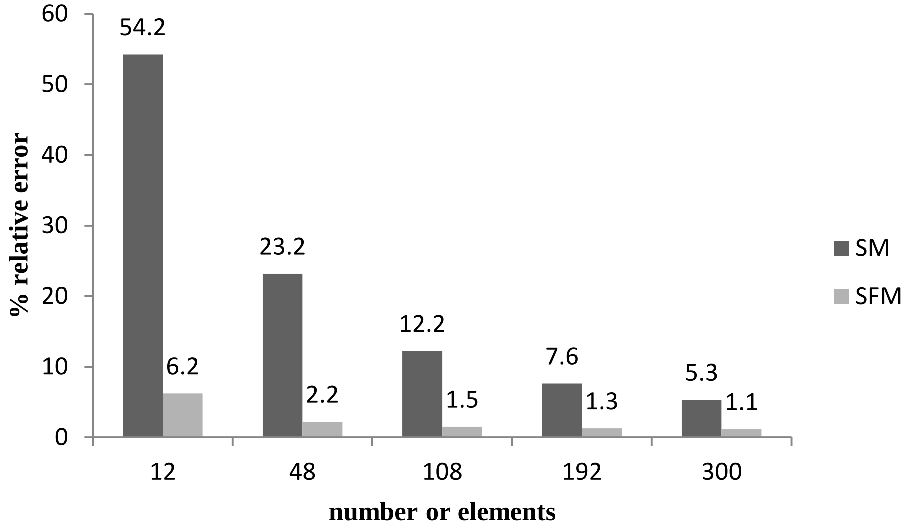
60
50
40
30
20
10
0
% relative error
54.2
6.2
23.2
2.2
12.2
1.5
7.6
1.3
5.3
1.1
12
48
108
192
300
number or elements
SM
SFM

Figure 9

Click here to download Figure FIG9.DOC.docx

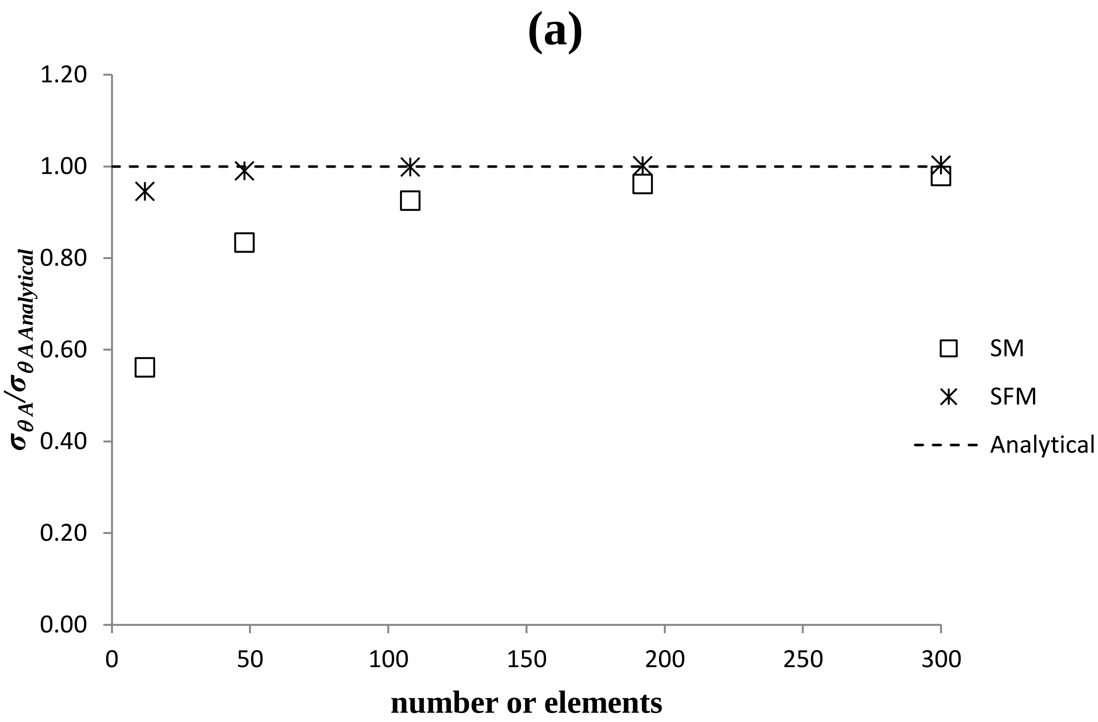

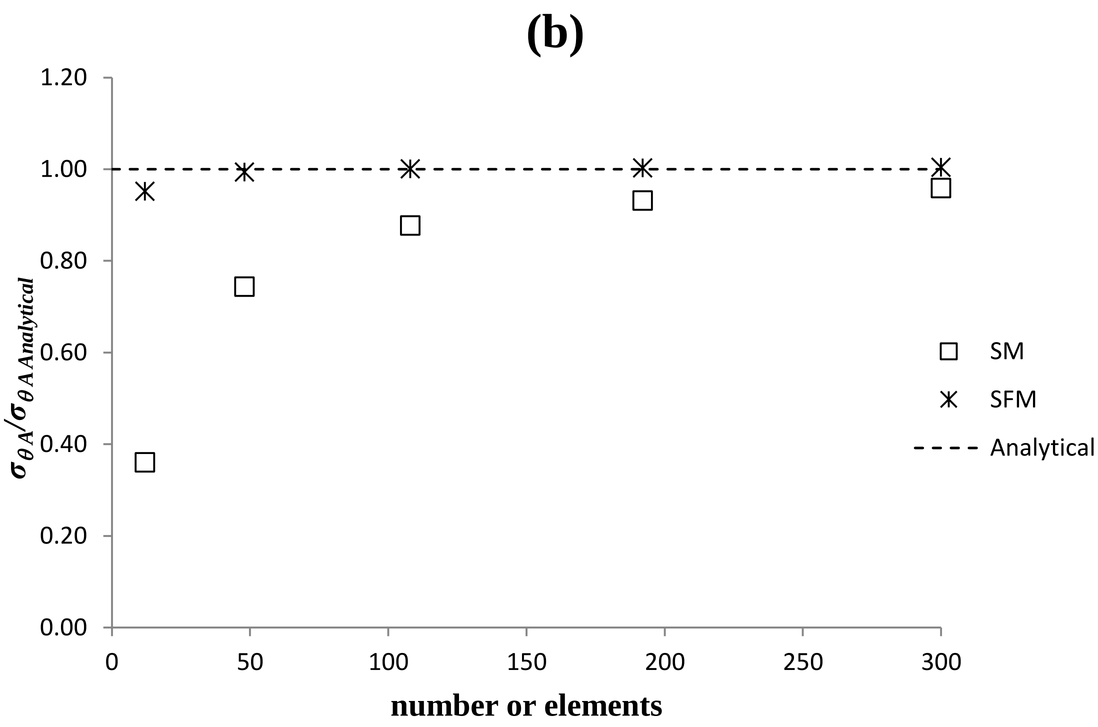

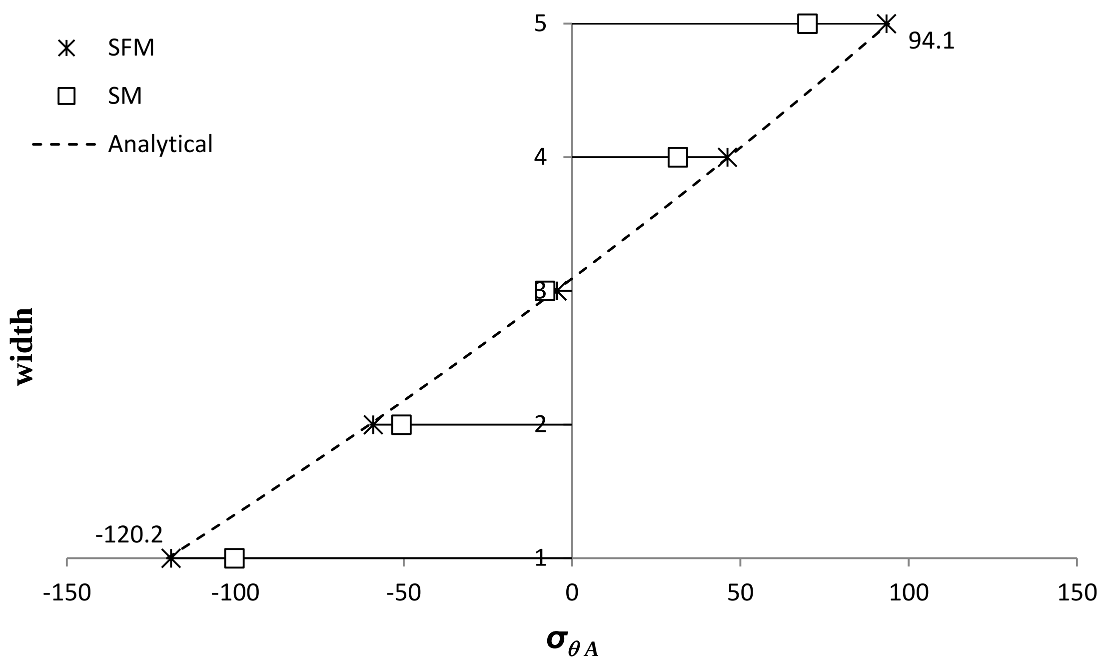
SFM
SM
Analytical
5
4
3
2
1
94.1
-120.2
width
-150
-100
-50
0
50
100
150
$\sigma_{\theta A}$

Figure 11 Click here to download Figure FIG11.DOC.docx